Journal of Receptors and Signal Transduction

ISSN: 1079-9893 (Print) 1532-4281 (Online) Journal homepage: https://www.tandfonline.com/loi/irst20

Synthesis, molecular docking, binding free energy calculation and molecular dynamics simulation studies of benzothiazol-2-ylcarbamodithioates as *Staphylococcus aureus* MurD inhibitors

Srikanth Jupudi, Mohammed Afzal Azam & Ashish Wadhwani

To cite this article: Srikanth Jupudi, Mohammed Afzal Azam & Ashish Wadhwani (2019) Synthesis, molecular docking, binding free energy calculation and molecular dynamics simulation studies of benzothiazol-2-ylcarbamodithioates as *Staphylococcus aureus* MurD inhibitors, Journal of Receptors and Signal Transduction, 39:3, 283-293, DOI: 10.1080/10799893.2019.1663538

To link to this article: https://doi.org/10.1080/10799893.2019.1663538

JOURNAL OF RECEPTORS AND SIGNAL TRANSDUCTION
2019, VOL. 39, NO. 3, 283–293
https://doi.org/10.1080/10799893.2019.1663538

Taylor & Francis
Taylor & Francis Group

RESEARCH ARTICLE

Synthesis, molecular docking, binding free energy calculation and molecular dynamics simulation studies of benzothiazol-2-ylcarbamodithioates as *Staphylococcus aureus* MurD inhibitors

Srikanth Jupudi[a], Mohammed Afzal Azam[a] and Ashish Wadhwani[b]

[a]Department of Pharmaceutical Chemistry, JSS College of Pharmacy, Ooty, India; [b]Department of Biotechnology, JSS College of Pharmacy, Ooty, India

ABSTRACT

A new series of benzothiazol-2-ylcarbamodithioate functional compounds **5a-f** has been designed, synthesized and characterized by spectral data. These compounds were screened for their *in vitro* antibacterial activity against strains of *Staphylococcus aureus* (NCIM 5021, NCIM 5022 and methicillin-resistant isolate 43300), *Bacillus subtilis* (NCIM 2545), *Escherichia coli* (NCIM 2567), *Klebsiella pneumoniae* (NCIM 2706) and *Psudomonas aeruginosa* (NCIM 2036). Compounds **5a** and **5d** exhibited significant activity against all the tested bacterial strains. Specifically, compounds **5a** and **5d** showed potent activity against *K. pneumoniae* (NCIM 2706), while compound **5a** also displayed potent activity against *S. aureus* (NCIM 5021). Compound **5d** showed minimum IC_{50} value of 13.37 μM against *S. aureus* MurD enzyme. Further, the binding interactions of compounds **5a-f** in the catalytic pocket have been investigated using the extra-precision molecular docking and binding free energy calculation by MM-GBSA approach. A 30 ns molecular dynamics simulation of **5d**/modeled *S. aureus* MurD enzyme was performed to determine the stability of the predicted binding conformation.

ARTICLE HISTORY
Received 23 June 2019
Revised 27 August 2019
Accepted 1 September 2019

KEYWORDS
Staphylococcus aureus MurD; molecular docking; molecular dynamics; antibacterial study; IC50

Abbreviations: ATP: adenosine triphosphate; DAP: 2,6-diaminopimelic acid; D-Glu: D-glutamic acid; IC_{50}: half maximal inhibitory concentration; MRSA: Methicillin-resistant *Staphylococcus aureus*; MIC: minimum inhibitory concentration; MurD: UDP-N-acetylmuramoyl-L-Ala:D-Glu ligase; MurNAc: N-acetyl muramic acid; UDP: uridine-5′-diphosphate; UMA: uridine-5′-diphosphate-N-acetylmueamoyl-l-alanine; RMSD: root mean square deviation; UMAG: UDP-N-acetylmuramoyl-L-alanine-D-glutamate; UDP-MurNAc: UDP-N-acetyl muramic acid

1. Introduction

Infections caused by methicillin-resistant *Staphylococcus aureus* (MRSA) are a leading cause of mortality and morbidity in humans around the world. It has emerged as a major public health threat and responsible for patient morbidity and mortality [1,2]. The alarming rise of *S. aureus* resistance to most of the antibiotics [3] has rendered the discovery of new antibacterial agents with potential novel mechanisms of action is critically important. Peptidoglycan (PG), part of the cell envelope of *S. aureus*, is essential to maintain the structural integrity of the cell wall. Its biosynthesis in bacteria is well understood and considered to be a potential target for the development of novel antibacterial drugs [4,5]. The ATP-dependent bacterial Mur ligases (MurC-F) catalyze the sequential addition of L-alanine, D-glutamic acid (D-Glu) and *meso*-2,6-diaminopimelic acid (*meso*-DAP) in Gram-negative or L-lysine in Gram-positive bacteria, and D-alanine-D-alanine dipeptide to UDP-N-acetyl muramic acid (UDP-MurNAc), to form UDP-MurNAc pentapeptide [6,7]. All Mur ligases share a common three-domain topology and most likely they operate by similar mechanisms of enzyme catalysis [8]. The multiple amino acid sequence alignment of Mur ligase orthologues and paralogues revealed relatively low overall homologies. However, the catalytic pocket binding residues are well conserved throughout the family [9–11]. Further, the cloned *S. aureus* MurD exhibited high percentage similarity to MurD proteins from *Escherichia coli* (54%), *Haemophilus influenzae* (55%), *Bacillus subtilis* (65%) and *Streptococcus pyogenes* (66%) [12].

Second in the series, *N*-acetylmuramoyl-L-alanine:D-glutamate ligase (MurD) catalyzes the ATP dependent phosphorylation of the UMA carboxylic acid. The resulting acyl-phosphate intermediate is then attacked by the amino group of the incoming D-Glu. The resulting tetrahedral high-energy intermediate collapses into the amide product, UDP-N-acetylmuramoyl-L-alanine-D-glutamate (UMAG) with elimination of inorganic phosphate [13,14]. Absence in human, ubiquity among bacteria and high specificity for D-amino acid make MurD an attractive target for inhibition of cell wall biosynthesis and hence development of new antibacterial agents [7,15]. MurD comprises three globular domains; the N-

CONTACT Mohammed Afzal Azam afzal9azam@hotmail.com, afzal@jssuni.edu.in Department of Pharmaceutical Chemistry, JSS College of Pharmacy, Ooty, Tamil Nadu, 643001, India

Supplemental data for this article can be accessed here.

terminal domain is responsible for the binding of UDP moiety of the UDP-*N*-acetylmuramoyl-L-alanine (UMA) substrate. The central domain binds the ATP while the C-terminal domain accounts for the fixation of the condensing amino acid or dipeptide residue.

Several phosphinate, α-aminophosphonate and *N*-acetylmuramic acid derivatives have been developed as tetrahedral transition state analog inhibitors of *E. coli* MurD but no promising results were obtained [16–19]. A series of non-phosphorylated and phosphorylated hydroxyethylamines have been investigated as inhibitors of whole cascade of Mur ligases (MurC to MurF) [20] with IC_{50} values in the micromolar range. Further, analogs of D-glutamic acid and substituted naphthalene-N-sulfonyl-D-glutamic acids were synthesized as potential transition state analog inhibitors of *E. coli* MurD [21–24]. The binding mode of these inhibitors provided important information for further leads optimization. Based on the virtual screening result, novel MurD ligase inhibitors possessing high potency were designed by incorporating the D-Glu moiety into the thiazolidin-4-one scaffold or its surrogate. Some of these designed inhibitors displayed weak antibacterial activity. Further, discovery of 5-benzylidenerhodanine and 5-benzylidenethiazolidine-2,4-dione-based *E. coli* MurD inhibitors [25,26] revealed details of the binding mode within the catalytic pocket. These efforts yielded useful information for the structure-based design of new generation of MurD inhibitors. Further, second generations of sulfonamide inhibitors possessing rigidified D-Glu mimetics have been synthesized [27,28]. These compounds exhibited significant improvement in *E. coli* MurD inhibitory activity compared to the first generation sulfonamide inhibitors. Some of these conformationally rigid mimetics displayed promising inhibitory activity when tested against the whole cascade of Mur ligases (MurD-MurF) [28].

The crystal structures of the MurD enzyme in complex with D-Glu derivatives have provided insights into the binding modes of these inhibitors [22,23]. Binding free energy calculations showed that the non-polar van der Waals interactions is the main driving force for the binding of these inhibitors [14,24,26,28,29]. Further, a D-Glu based dual inhibitor of *E. coli* and *S. aureus* MurD and MurE enzymes with promising activity against *S. aureus* and its methicillin-resistant strain (MRSA) was recognized and characterized by the crystallographic study [30]. This provided structural basis for the optimization and improvement in activity against MurD enzyme. Structure-based virtual screenings approaches have also been used to discover novel MurD inhibitors [24,30–32]. Unfortunately, the majority of these efforts have not yielded inhibitors with potent activity against both Gram-positive and Gram-negative bacteria (Figure 1)

Based on the *S. aureus* MurD structure [33] an *in silico* virtual screening campaign was performed. Compound **1** (Enamine T1827917) with incorporated 1–(3-hydroxyphenyl)ethylurea moieties was found to possess promising *S. aureus* MurD inhibitory activity with IC_{50} of 7 μM [34]. This compound demonstrated minimum inhibitory concentration (MIC) of 128 μg/ml against *S. aureus* NCIM 5021, *S. aureus* NCIM 5022 and *B. subtilis* NCIM 2545. In this study

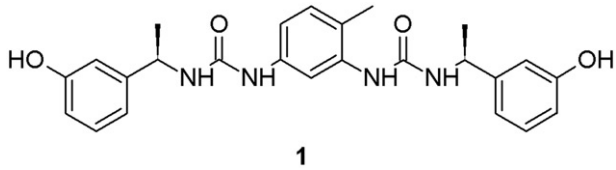

1

Figure 1. Represents chemical structure of virtual hit 1 (Enamine T1827917).

compound **1** was used as the starting point for the design of new *S. aureus* MurD inhibitors. Based on the molecular dynamics result of compound **1** [34], and with the aid of extra-precision experiments, different structural modifications were introduced into this molecule. As a first step we sought an appropriate substitute for one of the 1-[1–(3-hydroxyphenyl)ethyl]urea and linker 2-methylphenyl moiety. In lieu of 1-[1–(3-hydroxyphenyl)ethyl]urea and 2-methylphenyl, 2-phenoxyacetohydrazide or 2-hydrazinyl-2-oxoethyl 1,3-benzothiazol-2-ylcarbamodithioate were incorporated to improve the binding affinity with enzyme. Through several structure optimization cycles, benzothiazol-2-ylcarbamodithioate (**5a–f)** derivatives with favorable binding interactions with the modeled *S. aureus* MurD active site residues were designed for further study. The target compounds **5a–f** were synthesized as outlined in Scheme 1 and characterized by spectral data. The *in vitro* antibacterial screening of synthesized compounds was carried out against various pathogenic bacterial strains. *In vitro* enzyme inhibition assay was performed against *S. aureus* MurD enzyme to determine the IC_{50} values. Further, binding mode of designed compounds was investigated by the extra-precision molecular docking and molecular dynamics studies.

2. Experimental

2.1. Chemistry

Requisite chemicals were of reagent grade and were purified when required. All reactions were examined by thin layer chromatography (TLC) on Silica Gel F_{254} plates (Merck, Ltd., Germany). Melting points of the synthesized compounds were determined in open capillaries and are uncorrected. The infrared spectra were recorded either on a Shimadzu 8400S (Japan) or Perkin Elmer-Spectrum Two (United Kingdom) Fourier transform spectrometers and band positions are given in reciprocal centimeters (cm^{-1}). The ^{1}H and ^{13}C-NMR spectra were recorded on a Bruker AV-III 400 spectrometer (Germany) operating at 500 and 125 MHz, respectively, using dimethyl sulfoxide (DMSO-d_6) as solvent. The chemical shifts are reported in parts per million (ppm) using the solvent as internal standard. Mass spectra were recorded on electron impact (EI) JEOL GC-MATE II GC-MS spectrometer (USA) operating at 70 ev. Required 4-methoxybenzohydrazide, 4-methylbenzohydrazide, p-toluenesulfonyl hydrazide, 2-chlorobenzohydrazide, substituted 2-aminobenzothiazoles (**1a–c**) and 2-(chlorophenoxy)acetohydrazide (**3a–e**) were procured from Sigma-Aldrich. The intermediate, sodium dithiocarbamate salts **2a–c** were synthesized by reported method [35] and used without further purification. Synthetic routes for the titled compounds **5a–f** is represented in Scheme 1.

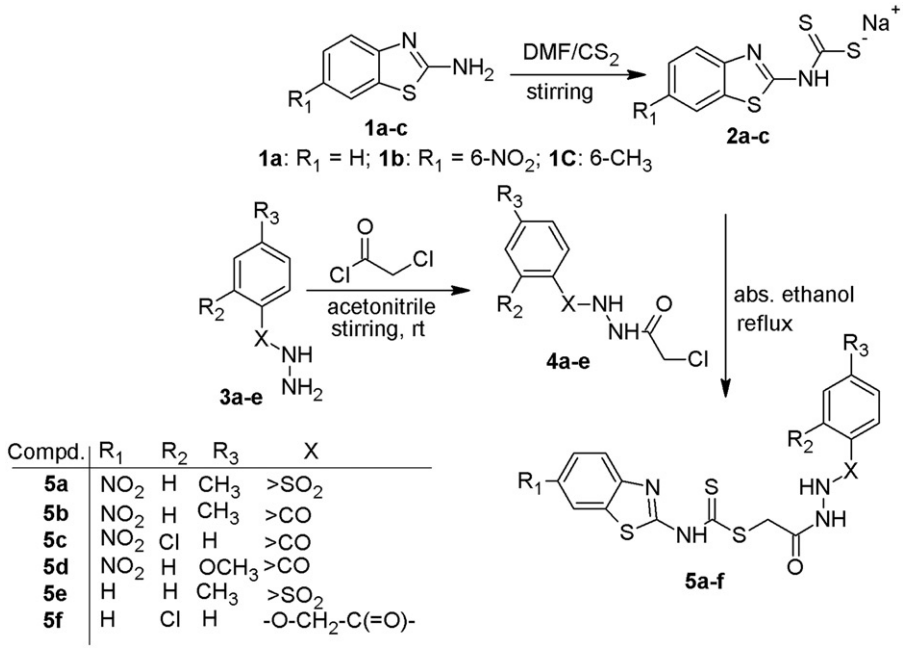

Compd.	R_1	R_2	R_3	X
5a	NO_2	H	CH_3	$>SO_2$
5b	NO_2	H	CH_3	>CO
5c	NO_2	Cl	H	>CO
5d	NO_2	H	OCH_3	>CO
5e	H	H	CH_3	$>SO_2$
5f	H	Cl	H	-O-CH_2-C(=O)-

Scheme 1. Synthesis and structures of titled compounds **5a–f**.

2.2. General procedure for the preparation of 2-oxo-2-[2-(phenylcarbonyl/sulfonyl)hydrazinyl]ethyl 1,3-benzothiazol-2-ylcarbamodithioates and 2-oxo-2-[2-(chlorophenoxyacetyl)hydrazinyl]ethyl 1,3-benzothiazol-2-ylcarbamodithioates (5a–f)

Compounds **4a–e** was prepared according to the previously reported method [36]

To a stirred mixture of 2/4-substitued benzohydrazides **3a–e** (0.66 mol) and K_2CO_3 (0.119 mol) in acetonitrile (100 ml), 2-chloroacetyl chloride (0.79 mol) was added dropwise at room temperature. Stirring was further continued overnight and the separated solid was filtered, washed thoroughly with water and dried to afford *N*′-(chloroacetyl)-(2/4-substituted benzohydrazides (**4a–c**)/2-chloro-*N*′-[(4-methylphenyl)sulfonothioyl]acetohydrazide (**4d**)/2-chloro-N′-[(2-chlorophenoxy)acetyl]acetohydrazide (**4e**) which were used for the next step without further purification. To a stirred warm solution of sodium dithiocarbamate salts **2a–c** (0.10 mol) in absolute ethanol (20 ml), appropriate hydrazides **4a–e** (0.12 mmol) was added in small portions during 15 min. The resulted reaction mixture was then heated under reflux for 18–24 h. After completion of reaction, excess solvent was evaporated under vacuum and to the residual mixture excess ice cold water was added. The solid thus separated was filtered, washed thoroughly with ice-cold water and recrystallized with appropriate solvent to yield titled compounds **5a–f**.

Synthetic route for the synthesized compounds **5a–f** is represented in Scheme 1.

*2-{2-[(4-Methylphenyl)sulfonyl]hydrazinyl}-2-oxoethyl(6-nitro-1,3-benzothiazol-2-yl) carbamodithioate (**5a**)*

Yield 63%. Solvent crystallization: ethanol. m.p.: 128–132 °C; Rf = 0.51; FT-IR (cm^{-1}): 3268, 3232 (NH), 3089 (Ar C–H), 2917, 2854 (CH_2), 1690, 1650 (>C=O), 1610 (>C=N), 1564 (>C=S), 1509, 1329 (NO_2), 1024 (>S=O); ^{1}H-NMR (DMSO-d_6): δppm 10.63 (s, 1H, NH), 10.50 (s, 1H, NH), 10.49 (s, 1H, NH), 8.29–8.03 (m, 3 H, ArH), 7.62– 7.47 (m, 4 H, ArH), 4.64 (s, 2 H, SCH_2), 2.51 (s, 3 H, CH_3); ^{13}C-NMR spectrum (DMSO-d_6): δppm 186.66 (>C=O), 173.56 (>C=S), 167.86, 159.07, 141.55, 132.16, 130.49, 130.39, 129.97, 122.96, 118.17, 117.34, 67.47 (SCH_2), 23.31 (CH_3); GC-MS (EI-TOF) *m/z* calculated for $C_{17}H_{15}N_5O_5S_4$ (497.59). Found: *m/z* 497.59 (M^+).

*2-[2–(4-Methylbenzoyl) hydrazinyl]-2-oxoethyl(6-nitro-1,3-benzothiazol-2-yl) carbamodithioate(**5b**)*

Yield 68%. Solvent crystallization: ethanol. m.p.: 248–250 °C; Rf = 0.49; FT-IR (cm^{-1}): 3268, 3178 (NH), 3073 (Ar C–H), 2924, 2854 (CH_2), 1689, 1650 (>C=O), 1625 (>C=N),1564 (>C=S), 1454 (–C=C–), 1517, 1329 (NO_2); ^{1}H-NMR (DMSO-d_6): δppm 11.39 (s, 1H, NH), 10.69 (s, 1H, NH), 10.33 (s, 1H, NH), 8.30–8.08 (m, 4 H, ArH), 7.85–7.29 (m, 3 H, ArH), 4.28 (s, 2 H, SCH_2), 2.50 (s, 3 H, CH_3); ^{13}C-NMR spectrum (DMSO-d_6): δppm 182.36 (>C=O), 167.78 (>C=O), 168.84 (>C=S), 154.53, 143.64, 129.71, 129.47, 128.10, 127.94, 122.51, 122.20, 119.64, 119.26, 118.17, 67.82 (SCH_2), 21.47 (CH_3). GC-MS (EI-TOF) *m/z* calculated for $C_{18}H_{15}N_5O_4S_3$ (461.53). Found: *m/z* 461.53 (M^+).

*2-[2–(2-Chlorobenzoyl) hydrazinyl]-2-oxoethyl (6-nitro-1,3-benzothiazol-2-yl) carbamodithioate (**5c**)*

Yield 51%. Solvent crystallization: ethanol. m.p.: 238–240 °C; Rf = 0.48; FT-IR (cm^{-1}): 3237, 3174 (NH), 3081 (Ar C–H), 2917, 2854 (CH_2), 1697, 1658 (>C=O), 1615 (>C=N), 1564 (>C=S), 1509, 1329 (NO_2), 1048 (Ar-Cl), 1016 (C-S); ^{1}H-NMR (DMSO-d_6): δppm 11.19 (s, 1H, NH), 10.92 (s, 1H, NH), 10.11 (s, 1H, NH), 8.29–7.98 (m, 4 H, ArH), 7.81–7.08 (m, 3 H, ArH), 4.58 (s, 2 H, SCH_2); GC-MS (EI-TOF) *m/z* calculated for $C_{17}H_{12}ClN_5O_4S_3$ (481.85). Found: *m/z* 481.95 (M^+).

*2-[2–(4-Methoxybenzoyl)hydrazinyl]-2-oxoethyl(6-nitro-1,3-benzothiazol-2-yl)carbamodithioate (**5d**)*

Yield 56%. Solvent crystallization: ethanol. m.p.: 272–275 °C; Rf = 0.51; FT-IR (cm^{-1}): 3245, 3215 (NH), 3081 (ArH), 2924, 2854 (CH_2), 1685, 1658 (>C=O), 1620 (>C=N), 1564 (>C=S), 1509(–C=C–), 1337 (NO_2), 844 (C-N), 1259,1048 (C-O-C); ^{1}H-NMR (DMSO-d_6): δppm 10.38 (s, 1H, NH), 10.22 (s, 1H, NH), 10.14 (s, 1H, NH), 8.69–8.09 (m, 3 H, benzothiazole), 7.89–7.84 (m, 4 H, ArH), 4.80 (s, 2 H, SCH_2), 3.86 (s, 3 H, OCH_3); ^{13}C-NMR spectrum (DMSO-d_6): δppm 172.26 (>C=O), 167.88 (>C=O), 167.27 (>C=S), 165.32, 165.32, 162.52, 159.07, 141.15, 132.06, 130.48, 130.39, 129.87, 122.46, 118.17, 67.46 (SCH_2), 55.86 (OCH_3). GC-MS (EI-TOF) *m/z* calculated for $C_{18}H_{15}N_5O_5S_3$ 477.53 (M^+). Found: *m/z* 481.65 (M^++4).

*2-{2-[(4-Methylphenyl) sulfonyl] hydrazinyl}-2-oxoethyl-1,3-benzothiazol-2-yl carbamodithioate(**5e**)*

Yield 69%. Solvent crystallization: ethanol. m.p.:180–184 °C; Rf = 0.51; FT-IR (cm^{-1}): 3214, 3162 (NH), 3010 (Ar C–H), 2917, 2846 (CH_2), 1680, 1658 (>C=O), 1630 (>C=N), 1548 (>C=S), 1509 (NH amide), 1337, 1165 (>S=O). ^{1}H-NMR (DMSO-d_6): δppm 10.58 (s, 1H, NH), 10.54 (s, 1H, NH), 10.32 (s, 1H, NH), 8.39–8.11 (m, 4 H, ArH), 7.72–7.38 (m, 4 H, ArH), 4.57 (s, 2 H, SCH_2), 2.49 (s, 3 H, CH_3); GC-MS (EI-TOF) *m/z* calculated for $C_{17}H_{16}N_4O_3S_4$ (452.59). Found: *m/z* 452.14 (M^+).

*2-{2-[(2-Chlorophenoxy)acetyl]hydrazinyl}-2-oxoethyl-1,3-benzothiazol-2-yl-carbamodithioate (**5f**)*

Yield 65%. Solvent crystallization: ethanol. m.p.: 126–130 °C; Rf = 0.55; FT-IR (cm^{-1}): 3214, 3182 (NH), 3049 (Ar C–H), 2924, 2854 (CH_2), 1679, 1642 (>C=O), 1618 (>C=N), 1572 (>C=S), 1611, 1486 (Ar –C=C–), 1235, 1024 (C-O-C); ^{1}H-NMR (DMSO-d_6): δppm 10.30 (s, 1H, NH), 10.28 (s, 1H, NH), 10.24 (s, 1H, NH), 7.98–7.29 (m, 4 H, ArH), 7.28– 6.97 (m, 4 H, ArH), 3.89 (s, 2 H, SCH_2), 3.60 (s, 2 H, OCH_2); ^{13}C-NMR spectrum (DMSO-d_6): δppm 185.26 (>C=O), 167.16 (>C=O), 166.63 (>C=S), 153.80,152.36, 130.53, 128.67,127.08, 126.23, 125.23, 124.42, 123.23, 123.12,122.69, 121.93, 114.63, 66.85 (OCH_2), 52.23 (SCH_2). GC-MS (EI-TOF) *m/z* calculated for $C_{18}H_{15}ClN_4O_3S_3$ (466.98). Found: *m/z* 466.35 (M^+).

2.3. In vitro *antibacterial screening of synthesized compounds*

2.3.1. Determination of minimum inhibitory concentration (MIC)

The antibacterial activity of the synthetic compounds against Gram-positive *S. aureus* (NCIM 5021 and NCIM 5022), methicillin resistant *S. aureus* (MRSA strain 43300), *B. subtilis* (NCIM 2545) and Gram-negative strains *E. coli* (NCIM 2567), *K. pneumoniae* (NCIM 2706) and *P. aeruginosa* (NCIM 2036) was assessed according to the guidelines of the Clinical Laboratories Standard Institute [37] to determine the MIC values. For each of the selected strains triplicate analyses were performed. MIC values were determined by microdilution broth technique using Mueller Hinton medium (Hi-media). Compounds **5a–f** was tested for their antibacterial activity in sterile dimethyl sulfoxide (DMSO). Sterile DMSO was used as a negative control while ciprofloxacin and gentamicin were used as control drugs (positive) in sterile DMSO. After incubation at 37 °C for 24 h, the 96 well plates were read for the MIC. MIC values are summarized in Table 1 and expressed as microgram per milliliter (μg/ml).

2.3.2. Enzyme inhibitory activity of S. aureus MurD ligase

The *S. aureus* MurD enzyme (ProFoldin, USA) inhibition assay was performed using the malachite green assay with slight modifications [38,39]. All of the experiments were performed in duplicate. The mixture with final volume of 50 μL contained: 500 mM TrisHCl, pH 8.0, 400 mM KCl, 10 mM DTT, 0.05% Triton X-100, 10 mM $MgCl_2$, 1 mM UDP-MurNAc-L-Ala, 5 mM D-Glu, 10 mM ATP, 5000 nM purified *S. aureus* MurD and 0.6 μL of different concentrations of each tested compound solution in dimethylsulfoxide (DMSO). The final concentration of DMSO was 5% (v/v) in all cases. The mixture was then incubated for 60 min at 37 °C and then quenched with Dye MPA3000. Incubated for 5 min and absorbance was measured at 650 nm and percentage inhibition was calculated. Percent inhibitions were calculated without the tested compounds and with 5% DMSO. IC_{50} values were determined using the GraphPad PRISM.

3. Computational analysis

3.1. Molecular docking and binding free energy calculation (MM-GBSA)

The 3 D-structures of compounds **5a–f** were prepared using the builder panel in Maestro 11.5 (Schrodinger software suite 2018–1, LLC, New York, NY, USA) and subsequently optimized with LigPrep [40]. The molecular docking was performed in extra-precision (XP) mode with Glide without applying any constraints. The binding free energies were calculated using VSGB 2.0 energy model (MM-GBSA approach) and prime [41,42] with OPLS3 force field [43]. In this study, we used the earlier prepared grid box of modeled *S. aureus* MurD protein [33]. The low energy conformation of all prepared ligands were docked and their binding free energies were computed employing the protocols described earlier [33].

Table 1. Antibacterial activity of synthesized compounds **5a–f** against Gram-positive and Gram-negative bacteria.

	Minimum inhibitory concentration (μg/ml)*						
Compound	[a]*S. a*	[b]*S.a*	[c]*S. a*	[d]*B. s*	[e]*K. p*	[f]*P. a*	[g]*E. c*
5a	2	32	64	16	2	256	16
5b	128	128	128	>256	64	128	64
5c	64	128	256	128	16	256	32
5d	32	32	64	64	4	128	16
5e	128	128	128	128	64	128	>256
5f	64	64	128	128	32	256	32
Ciprofloxacin	2	2	32	2	2	2	2
Gentamicin	8	8	19.5	8	1	1	1

*average of three independent determinations.
[a]S. a: Staphylococcus aureus NCIM 5021; [b]S. a: Staphylococcus aureus NCIM 5022; [c]S. a: Staphylococcus aureus ATCC 43300 (MRSA); [d]B. s: Bacillus subtilis NCIM 2545; [e]K. p: Klebsiella pneumoniae NCIM 2706; [f]P. a: Pseudomonas aeruginosa NCIM 2036; [g]E. c: Escherichia coli NCIM 2567.

3.1.2. MD Simulation

The extra-precision-docked structure of compound **5d**/*S. aureus* MurD modeled protein complex was used as starting structure for MD simulation [41] using the Desmond software with OPLS3 force field [43]. The complex was solvated with explicit TIP4P [44,45] water in an orthorhombic box allowing for a 10 Å buffer region between protein atoms and box sides. The solvated system was neutralized by adding 5 counter sodium ions. Finally, the modeled system contains approximately 56566 atoms, 16485 water molecules, and a final box volume of 1186013 $Å^3$. Prior to MD simulation whole system was minimized with OPLS3 [43] force field using 200 steepest descent, followed by 1000 steps of conjugate gradient until a gradient threshold of 25 kcal/mol/Å was reached. The long range electrostatic interactions were treated by using the Particle-mesh-Ewald method [46] at a tolerance of 1e-09. For van der Waals and Coulomb interactions a cutoff radius of 9 Å was applied. The minimized system was then simulated for 30 ns under an isothermal-isobaric ensemble (NPT) at a constant temperature of 300 K and a constant pressure of 1 bar. A Nose-Hoover thermostat [47] and Martyna-Tobias-Klein barostat [48] were used to maintain temperature and pressure, respectively. A multiple time step RESPA integration algorithm was used for the bonded, near nonbonded, and far nonbonded interactions, with time steps of 2, 2, and 6 fs, respectively. The MD time step was taken to be 2 fs for the overall simulations, and data were collected every 100 ps. The 3 D structures and trajectory were visually analyzed using the Maestro graphical interface.

4. Results and discussion

4.1. Chemistry

The synthetic routes for title compounds **5a–f** are outlined in Scheme 1. Solution of benzothiazoles (**1a-c**) in DMF are stirred with carbon disulfide in the presence of sodium hydroxide. The obtained sodium salts of benzothiazol-2-ylcarbamodithioates (**2a-c**) are further treated with appropriate *N*′-(chloroacetyl)-(2/4-substituted benzohydrazides (**4a-c**)/2-chloro-*N*′-[(4-methylphenyl)sulfonothioyl]acetohydrazide (**4d**)/2-chloro-*N*′-[(2-chlorophe-noxy)acetyl]ace tohydrazide (**4e**) in refluxing absolute ethanol to yield title compounds **5a–f** in good yields.

The structures of the new synthesized compounds were confirmed by IR and NMR (^{1}H and ^{13}C) and mass spectroscopy. In the infrared spectra of compounds **5a–f** characteristic absorption bands of –NHNH– and –NH– appeared in the region 3162 to 3268 cm^{-1}. The >C=O and benzothiazole >C=N groups showed stretching absorption bands in the region between 1642 to 1697 $cm^{-1}$and 1610 to 1630 cm^{-1}, respectively. In the ^{1}H-NMR spectra of compounds **5a–f** three singlet signals appeared in the region δ 10.11 to 11.39 ppm are assigned to the –CONHNH- and -CSNH- fragment protons. The singlet signals observed in the region δ 3.89 to 4.80 ppm are ascribed to two protons of $–SCH_2$- fragment. The ^{13}C NMR spectra of compounds **5b, 5d** and **5f** exhibited two singlet signals for >C=O carbons in the region δ 167.16 to 185.26 ppm whereas one >C=O carbon of compound **5a** appeared at δ 186.66 ppm. The >C=S carbon signal in these compounds appeared in the range δ 166.63 to 173.56 ppm. All aromatic protons of these compounds appeared at their expected positions. The mass spectra showed molecular ion peaks which are in conformity with their molecular formula (see experimental also Supplementary Figure S1a-i).

4.2. Determination of minimum inhibitory concentration (MIC)

The antibacterial activity of the synthesized compounds was assayed by two-fold broth micro-dilution method, following the procedures of the Clinical and Laboratory Standards Institute [37]. The result of these compounds showing antibacterial activity is given in Table 1. MIC values of synthesized compounds are compared with the standard drugs ciprofloxacin and gentamicin. Tested compounds **5a**, **5d**, and **5f** belonging to the benzothiazol-2-ylcarbamodithioate series displayed promising inhibitory activity against Gram-positive *S. aureus* NCIM 5021 and *S. aureus* NCIM 5022 with MIC values in the range 2–64 μg/ml compared to the standard drugs ciprofloxacin and gentamicin (MICs, 2 and 8 μg/ml, respectively against both strains). Among these tested compounds, **5a** possessing 4-methylbenzenesulfonohydrazide moiety and $–NO_2$ group on position six of benzothiazole ring showed maximum inhibitory activity (MIC, 2 μg/ml) against *S. aureus* NCIM 5021 compared to the standard drugs ciprofloxacin (MIC, 2 μg/ml) and gentamicin (MIC, 8 μg/ml). Compounds **5a** and **5d** also showed maximum inhibitory activity against both *S. aureus* NCIM 5022 (MIC, 32 μg/ml in both cases) and methicillin resistant *S. aureus* ATCC 43300 (MIC, 64 μg/ml in both cases) Gram-positive bacteria. While other tested compounds were observed to be less active (MIC, 128 to 256 μg/ml) or inactive (>256 μg/ml) against *S. aureus* ATCC 43300. It is evident that among benzothiazol-2-ylcarbamodithioates, presence of electron withdrawing $–NO_2$ group on position six of the benzothiazole ring and electron releasing substituents $–CH_3$ or $–OCH_3$ on position four of phenyl ring is optimal for the activity against methicillin resistant *S. aureus* ATCC 43300.

Among all the tested compounds, benzothiazol-2-ylcarbamodithioates **5a** and **5d** exhibited maximum inhibitory activity against *B. subtilis* NCIM 2545 (MIC, 16 μg/ml). Compound **5d** also showed significant inhibitory activity against this strain with an MIC value of 64 μg/ml. Other tested compounds were observed to be either less active (128 μg/ml) or inactive (MIC >256 μg/ml) against this microorganism. Further, compounds **5a–f** exhibited promising antibacterial activity against Gram-negative *K. pneumoniae* NCIM 2706 (Table 1, MIC, 2 to 64 μg/ml). Among all the tested compounds, **5a** and **5d** exhibited potent inhibitory activity against this bacterial strain, respectively with MIC values of 2 and 4 μg/ml, compared to the standard drugs ciprofloxacin (2 μg/ml) and gentamicin (1 μg/ml). While all other tested compounds were observed to be either less active or inactive against this strain. On the other hand, tested

compounds showed variable activity against *E. coli* NCIM 2567. Among the six tested compounds, five compounds exhibited significant inhibitory activity against *E. coli* NCIM 2567 (MIC, 16 to 64 μg/ml). Maximum inhibitory activity was observed for compounds **5a** and **5d** with MIC value of 16 μg/ml in both cases. It is evident from the above result that compounds **5a** and **5d** possess fairly good inhibitory activity against all the tested strains of Gram-positive and Gram-negative bacteria except *P. aeruginosa* NCIM 2036.

4.3. Enzyme inhibitory activity of S. aureus MurD ligase

In vitro inhibitory potency for five selected compounds was determined using *S. aureus* MurD enzyme (ProFoldin, USA) (Table 2). The tested compounds displayed IC_{50} values in the range 13.37–79.27 μM. Among the assayed compounds, two compounds namely **5a** and **5d** belonging to the benzothiazol-2-ylcarbamodithioate series were found to inhibit *S. aureus* MurD enzyme with IC_{50} values of 22.33 and 13.37 μM, respectively. Other three compounds **5c**, **5e** and **5f** belonging to this series displayed moderate inhibition with IC_{50} values of 52.16, 75.34 and 79.27 μM, respectively. It is evident from above result that the presence of electron withdrawing -NO_2 group on position six of the benzothiazole ring and electron releasing groups (-CH_3 and -OCH_3) on position four of the phenyl ring are beneficial for the inhibitory activity.

4.4. Computational analysis

Compounds **5a–f** interaction energies (Table 3) into the catalytic pocket of modeled *S. aureus* MurD enzyme were calculated to get insight into their binding modes and affinity. Comparison of the XP-Glide docking poses of compounds showed similar interactions dominated by the hydrogen bond, salt bridge, π-π stacking and π-cation stacking interactions with conserved residues Lys19, Ser20, Ser168, Phe170, His192, His196, Asp426 and Glu432 (Supplementary Table S1 and Figure S2(a–c)).

It can be seen in Figure 2(b) that the high active compound **5d** (IC_{50} 13.37 μg/ml) is placed well within the catalytic pocket and occupied all three domains of the catalytic pocket. It formed five hydrogen bonds with the key binding residues. Specifically, the carbonyl oxygen of 4-methoxybenzohydrazide moiety formed two hydrogen bonds one each with the side chain NH of Lys19 (>C=O···HN, 2.09 Å) and the backbone OH of Ser20 (>C=O···HN, 1.95 Å), present in the N-terminal domain of catalytic pocket. NH of -S-CH_2-CO-NH- fragment formed hydrogen bond with the side chain > C=O of Glu432 (NH···O=C<, 1.98 Å), while NH attached to the 6-nitrobenzothizole ring established a hydrogen bond with the side chain carboxylate oxygen of Asp426 (NH···$^{-}$O-C(=O)–, 2.50 Å) present in the C-terminal domain. Further, oxygen of nitro group formed a hydrogen bond with the side chain NH of His196 (–(O)N = O···HN, 2.29 Å) present in the ATPase domain of the catalytic pocket.

Like **5d**, another high active compound **5a** (IC_{50}, 22.33 μg/ml) also occupied all three domains of catalytic pocket and exhibited a total of five hydrogen bonds (Figure 2(a)). The nitro group present on position six of benzothiazole ring accepted a hydrogen bond from the side chain NH of Lys77 ((O)N=O···NH, 2.14 Å), while another oxygen of this nitro group formed a salt bridge interaction with the same residue. This nitro group also exhibited a π-cation interaction with the side chain imidazole ring of His192. The NH attached to the benzothizole ring formed a hydrogen bond with the side chain carbonyl oxygen of Glu432 (NH···O=C<, 2.15 Å), whereas both NH of –CO-NH-NH-CO- fragment formed one hydrogen bond each with the side chain > C=O of Thr430 (NH···O=C<, 2.14 Å) and the backbone carbonyl oxygen of Ala18 (NH···O=C<, 1.94 Å). The carbonyl oxygen of –NH–CO–CH_2–S– fragment accepted a hydrogen bond from the backbone NH of Gly80 (>C=O···HN, 1.91 Å).

Table 2. IC_{50} (μM) values of some selected compounds against *S. aureus* MurD enzyme.

Compound	IC50(μM) *S. aureus* MurD
5a	22.33 ± 0.93
5c	52.16 ± 0.56
5d	13.37 ± 0.58
5e	75.34 ± 0.81
5f	79.27 ± 0.53

Table 3. Extra-precision docking score and binding free energy between compounds **5a–f** and modeled *S. aureus* MurD protein computed by the MM-GBSA approach (kcal/mol).

Compound	[a]G_{score}	[b]G_{emodel}	[c]G_{energy}	[d]ΔG_{Coul}	[e]ΔG_{Lipo}	[f]ΔG_{Solv}	[g]ΔG_{vdW}	[h]ΔG_{bind}
5a	−5.89	−88.96	−62.41	−50.16	−15.43	52.70	−56.30	−64.18
5b	−5.3	−85.08	−61.65	−34.98	−15.30	19.19	−36.72	−93.22
5c	−5.7	−94.85	−66.22	−42.14	−17.45	25.17	−47.19	−91.43
5d	−5.31	−85.80	−58.65	−26.84	−31.20	54.38	−87.15	−85.33
5e	−4.41	−73.76	−52.87	−47.27	−27.47	36.80	−70.52	−79.73
5f	−6.09	−83.19	−58.55	−88.92	−31.36	78.92	−86.67	−95.32

[a]Glide score; [b]Glide model energy; [c]Glide energy; [d]Coulomb energy; [e]hydrophobic energy (nonpolar contribution estimated by solvent accessible surface area); [f]electrostatic solvation energy; [g]van der Waals energy; [h]Free energy of binding.

The binding strength of compounds **5a–f** with modeled *S. aureus* MurD protein is determined by the binding free energy (ΔG_{bind}) (Table 3). The calculated ΔG_{bind} values are in the range −64.18 to −95.32 kcal/mol. The van der Waals ($\Delta G_{vdW,}$ −36.72 to −87.15 kcal/mol) and electrostatic interaction (ΔG_{Coul}, −26.84 to −88.92 kcal/mol) energy terms are observed to be the major contributors for the inhibitors binding. Electrostatic solvation energy (ΔG_{Solv}, 19.19 to 78.92 kcal/mol) term disfavors the binding of other inhibitors to the modeled *S. aureus* MurD protein. It is also evident from result that there is little favorable contribution from non-polar solvation (ΔG_{Lipo}, −15.30 to −31.36 kcal/mol) energy term. Further, it should be noted that ΔG_{vdW} is much stronger than ΔG_{Coul}, indicating that van der Waals interaction is the driving force for the inhibitor binding. This is in agreement with the earlier report [14,24,26,28,29] and also with the Glide Emodel (G_{emodel}, −73.76 to −94.85 kcal/mol) having significant weighting of the force field.

In order to validate the stability and to get insight into the binding mode, a 30 ns MD simulation was performed for **5d**/*S. aureus* MurD modeled protein complex. During MD simulation the RMSD values of protein all Cα and backbone atoms increased during equilibration upto 16 ns and then

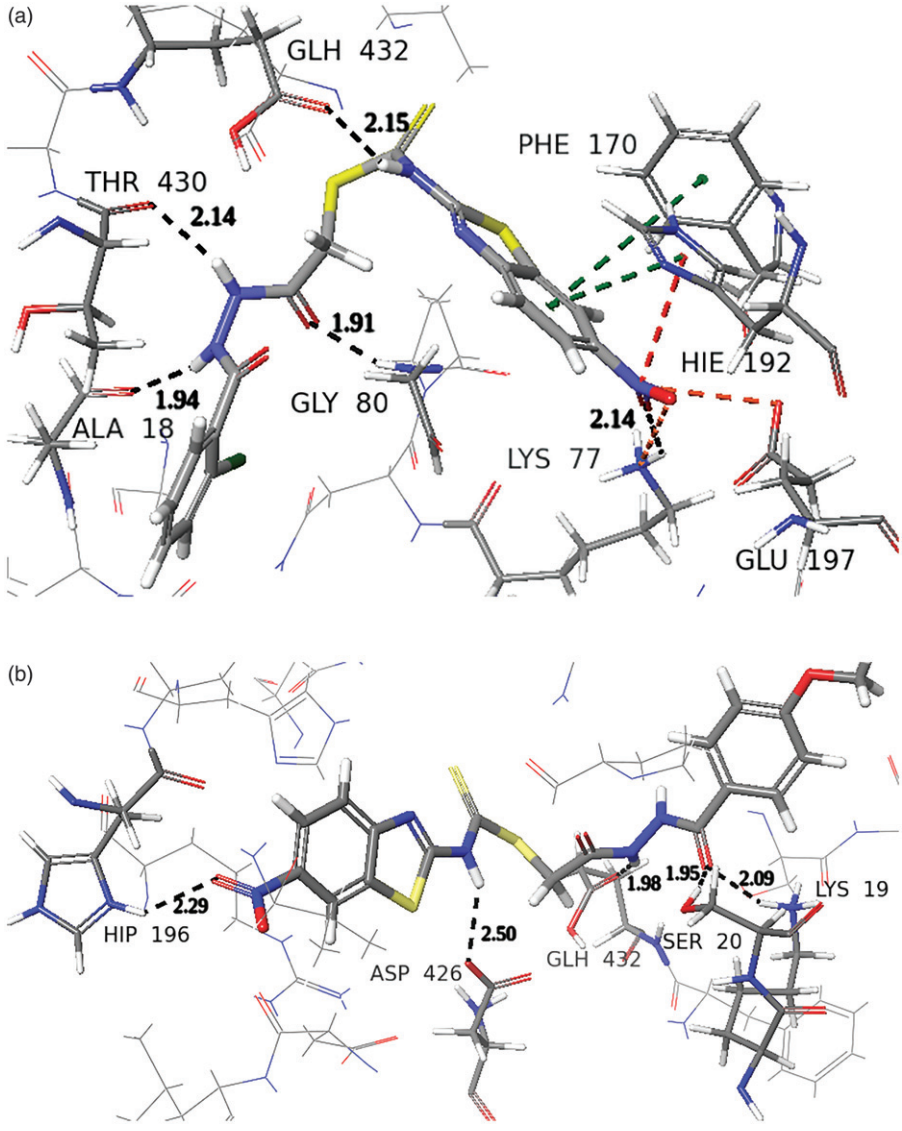

Figure 2. Represents extra-precision docking pose of compounds (a) **5a** and (b) **5d** in the catalytic pocket of modeled *S. aureus* MurD protein.

stabilized in the range 2.04–2.51 Å and 2.07–2.54 Å, respectively (Figure 3(a)). This indicated less conformational changes in protein structure during simulation. After 16 ns the mean radius of gyration (rGYr) fluctuation of the backbone (blue diamond) and Cα (red circle) atoms (Supplementary Figure S3) was observed to be low (0.40 and 0.42, respectively) which further indicated the low degree of flexibility in the protein complex. The ligand RMSD witness conformational variation upto 10 ns, stabilized between 10 and 30 ns and copes well with the tendency of binding pocket residues RMSD (Supplementary Figure S4a). The mean root mean square fluctuation (RMSF) values of Cα and backbone atoms of catalytic pocket binding residues was observed to be in the range 0.68 to 1.27 and 0.69 to 1.28 Å, respectively (Figure 3(b)), indicating no significant fluctuations of these residues. Residues Glu232-Leu234 which are present on the loop (Tyr223-Thr238) and connecting two β-sheets (Leu239-Phe241) exhibited maximum RMSFs of Cα (2.38–3.17 Å) and backbone (2.66–3.16 Å) atoms.

Analysis of the MD trajectory of **5d**/*S. aureus* MurD modeled protein complex revealed hydrogen bonding, salt bridge, π-cation and π-π stacking interactions (Figure 3(c,d) also Supplementary Figure S4) between amino acid stretches Lys19-Glu197 and Thr330-Arg434. However, no interaction was observed in the region Asn198-Ala329. Among the five hydrogen bonds observed in extra-precision docking, three (Lys19 >C=O···HN, Asp426 NH···$^{-}$O-C(=O)-, and His196 -(O)N=O···HN) are preserved during 15–62% of MD trajectory. Precisely, oxygen of nitro group accepted a direct (36% of the MD trajectory) and water mediated (24% of the MD the trajectory) hydrogen bonds from His196. The nitrogen of this nitro group also showed a moderate frequency (33% of the MD trajectory) salt bridge and a low frequency (17% of the MD the trajectory) water mediated hydrogen bond interactions with Asp42. Additionally, a moderate frequency (26% of the MD trajectory) π-cation interaction was observed between nitrogen of the nitro group and imidazole ring of His192. The carbonyl oxygen of –CH_2–CO–NH–NH– fragment accepted a high frequency (58% of the MD the trajectory) hydrogen bond from Gln171, while the nitrogen of benzothiazole ring accepted a medium frequency (47% of the MD the trajectory) water mediated hydrogen bond from the same

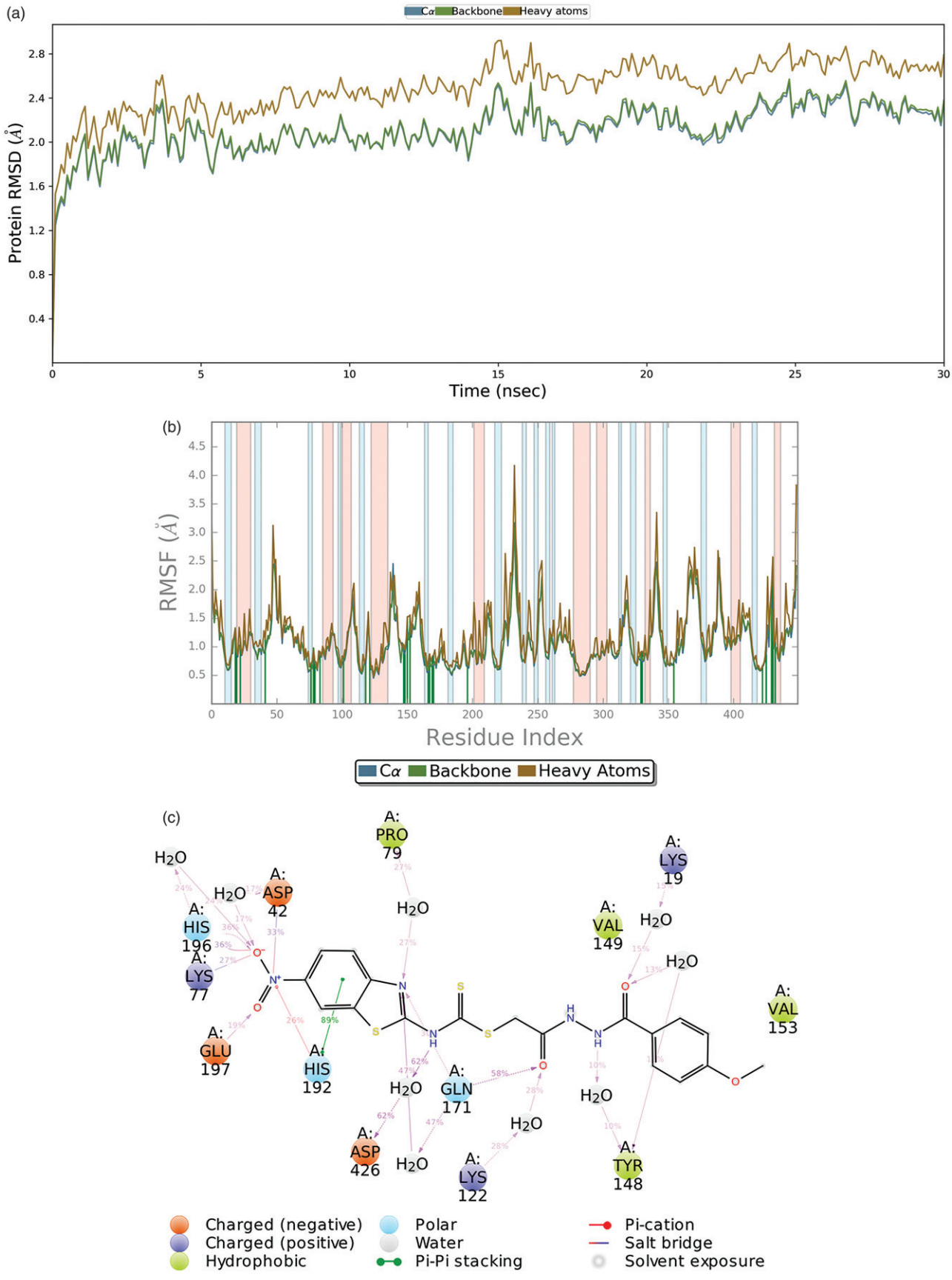

Figure 3. Plot represent (a) RMSD (Å) of the simulated positions of modeled *S. aureus* MurD protein Cα and backbone atoms from those in the initial structure. (b) RMSF profile of modeled *S. aureus* MurD residues (c) interaction of compound **5d** with different residues of modeled *S. aureus* MurD protein (d) interaction fraction profile of compound **5d** with different residues of modeled *S. aureus* MurD during MD simulation.

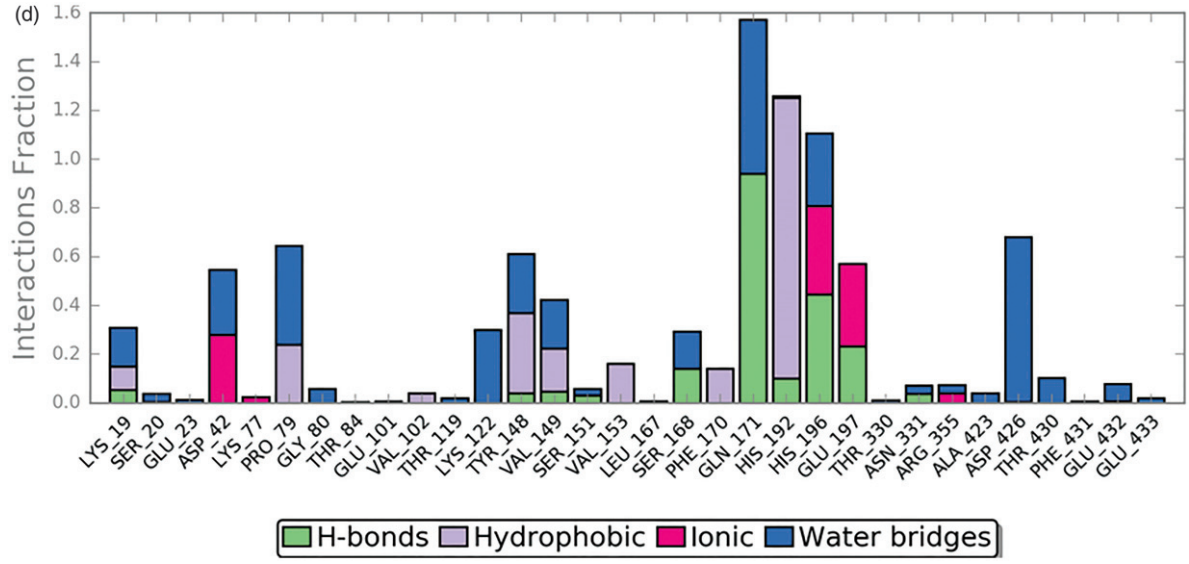

Figure 3. Continued.

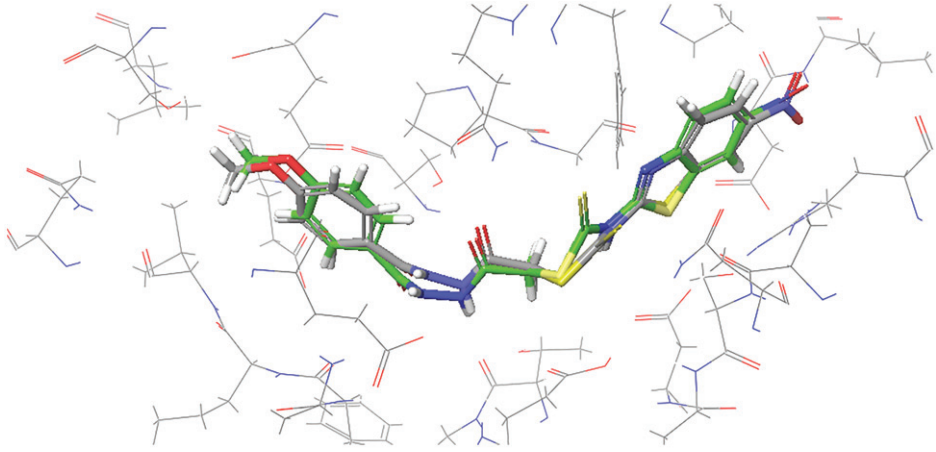

Figure 4. Superimposition of conformations of docked pose of compound **5d** and MD pose [RMSD: 0.552 Å].

residue. A high frequency (89% of the MD trajectory) π-π stacking was observed between the benzo part of the benzothiazole ring and the imidazole ring of His192. Inhibitor **5d** also exhibited low to moderate frequency hydrogen bonds with Lys77, Lys122, Tyr148 and Glu197 residues. It is evident from above result that Glu171, His192, His196 and Asp426 played crucial role for the stabilization of inhibitor **5d** within the catalytic pocket.

The rGyr which measures the extendedness of ligand was in the range 4.9–5.9 Å (Supplementary Figure S5), indicating the stability of **5d** within the catalytic pocket throughout the 30 ns MD simulation. The lower RMSD value (0.9–2.2 Å) during 15–30 ns of MD simulation further confirms the less conformational flexibility and stability of **5d** during simulation. The solvent accessible surface area (SASA) of inhibitor **5d** increased up to 15 ns (20–100 $Å^2$) and then stabilized in the range 50–110 $Å^2$, indicating no significant change in the binding pocket volume during MD simulation. Further, the inhibitor also showed low polar surface area (PSA) (195–235 $Å^2$), indicating the complete burial of linker between 6-nitrobenzothiazole and 4-methoxyphenyl rings within the hydrophilic pocket (Supplementary Figure S6). Superposition of the conformations of **5d** after MD simulation and best docking pose showed similar orientation with RMSD of 0.552 Å (Figure 4), indicating the rationality and validity of the extra-precision docking model.

4.5. Calculation of pharmacokinetic and toxicological properties

Absorption, distribution, metabolism, excretion and toxicity (ADMET) properties of synthesized compounds **5a–f** was computed by QikProp module incorporated in Schrödinger software suite 2018–1. All compounds obeyed Lipinski's rule of five with 0 to 1 violation, showing the drug like property of these molecules (Supplementary Table S2). The predicted central nervous system (CNS) activity of these molecules was within the recommended range (−2 as inactive and +2 as active) indicating lack of CNS activity. The Polar Surface Area (PSA, indicative of Van der Waals surface area of polar nitrogen and oxygen atoms) ranges between 120.3 to 167.1 $Å^2$ and is within the recommended range (7–200 $Å^2$). The computed QPlogPo/w values are within range 1.82 to 4.41 indicating the favorable oral absorption of these molecules.

Further, the predicted apparent Caco-2 cell permeability of the molecules are in the ranges 53.05 to 343.4 nm/sec, indicating non-active transport of these molecules. The predicted IC_{50} values for the blockage of human ether-a-go-go (HERG) K^+ channels (QPlogHERG) is observed to be in the range −2.84 to −4.81, indicating the safety of these molecules. The solvent accessible surface area (SASA) of these molecules is in the range 708.89 to 778.62 $Å^2$ indicating the burial of these molecules within the catalytic pocket.

5. Conclusion

In the present study, we designed six compounds **5a–f** in the catalytic pocket pocket of *S. aureus* MurD enzyme. These compounds are synthesized and characterized by spectral data. *In vitro* antibacterial activity of these compounds was evaluated against strains of *S. aureus* (NCIM 5021, NCIM 5022 and methicillin-resistant isolate 43300), *B. subtilis* (NCIM 2545), *E. coli* (NCIM 2567), *K. pneumonia* (NCIM 2706) and *P. aeruginosa* (NCIM 2036). Compounds **5a** and **5d** belonging to the benzothiazol-2-ylcarbamodithioate series exhibited significant inhibitory activity against all tested bacterial strains. Specifically, compounds **5a** and **5d** showed potent activity against *K. pneumonia* (NCIM 2706). Compound **5a** also displayed potent activity against *S. aureus* (NCIM 5021). An IC_{50} value of selected compounds was determined by malachite green assay method. Compound **5d** showed minimum IC_{50} value of 13.37 μM against *S. aureus* MurD enzyme. Further, the binding modes of compounds **5a–f** have been studied using molecular docking and binding free energy calculation by MM-GBSA approach. The major contributors for the inhibitors binding were observed to be van der Waals and electrostatic interaction energy terms. In most of the active compounds electrostatic solvation energy term disfavors the binding to the modeled *S. aureus* MurD protein. Further, van der Waals interaction is observed to be the driving force for the inhibitor binding. A 30 ns molecular dynamics (MD) simulation of **5d**/modeled *S. aureus* MurD complex was performed to validate the stability.

Disclosure statement

No potential conflict of interest was reported by the authors.

Funding

The study was financially supported by the Science and Engineering Research Board (SERB), Government of India for the financial support (No. EMR/2016/002981).

ORCID

Srikanth Jupudi http://orcid.org/0000-0001-8005-1905
Mohammed Afzal Azam http://orcid.org/0000-0001-9770-9371
Ashish Wadhwani http://orcid.org/0000-0001-6844-7069

References

[1] Loewen K, Schreiber Y, Kirlew M, et al. Community-associated methicillin-resistant *Staphylococcus aureus* infection. Can Fam Physician. 2017;63(7):512–520.
[2] Boucher HW, Corey GR. Epidemiology of methicillin-resistant *Staphylococcus aureus*. Clin Infect Dis. 2008;46(S5):S344–S349.
[3] Macmorran E, Harch S, Athan E, et al. The rise of methicillin resistant *Staphylococcus aureus*: now the dominant cause of skin and soft tissue infection in Central Australia. Epidemiol Infect. 2017;145(13):2817–2826.
[4] Bugg TDH, Braddick D, Dowson CG, et al. Bacterial cell wall assembly: still an attractive antibacterial target. Trends Biotechnol. 2011;29(4):167–173.
[5] Gautam A, Vyas R, Tewari R. Peptidoglycan biosynthesis machinery: a rich source of drug targets. Crit Rev Biotechnol. 2011;31(4):295–336.
[6] Barreteau H, Kova A, Boniface A, et al. Cytoplasmic steps of peptidoglycan biosynthesis. FEMS Microbiol Rev. 2008;32(2):168–207.
[7] El Zoeiby A, Sanschagrin F, Levesque RC. Structure and function of the Mur enzymes: development of novel inhibitors. Mol Microbiol. 2003;47(1):1–12.
[8] Smith CA. Structure, function and dynamics in the Mur family of bacterial cell wall ligases. J Mol Biol. 2006;362(4):640–655.
[9] Gordon E, Flouret B, Chantalat L, et al. Crystal Structure of UDP-*N*-acetylmuramoyl-l-alanyl-d-glutamate:*meso*-Diaminopimelate ligase from *Escherichia coli*. J Biol Chem. 2001;276(14):10999–11006.
[10] Ikeda M, Wachi M, Jung HK, et al. Homology among MurC, MurD, MurE and MurF proteins in *Escherichia coli* and that between *Escherichia coli* MurG and a possible MurG protein in *Bacillus subtilis*. J Gen Appl Microbiol. 1990;36(3):179–187.
[11] Bouhss A, Dementin S, Parquet C, et al. Role of the ortholog and paralog amino acid invariants in the active site of the UDP-MurNAc-L-alanine:D-glutamate ligase (MurD). Biochemistry. 1999;38(38):12240–12247.
[12] El-Sherbeini M, Geissler WM, Pittman J, et al. Cloning and expression of *Staphylococcus aureus* and Treptococcus pyogenes murD genes encoding uridine diphosphate N-acetylmuramoyl-L-alanine:D-glutamate ligases. Gene. 1998;210(1):117–125.
[13] Bertrand JA, Auger G, Fanchon E, et al. Crystal structure of UDP-N-acetylmuramoyl-L-alanine:D-glutamate ligase from *Escherichia coli*. EMBO J. 1997;16(12):3416–3425.
[14] Perdih A, Kotnik M, Hodoscek M, et al. Targeted molecular dynamics simulation studies of binding and conformational changes in *E. coli* MurD. Proteins. 2007;68(1):243–254.
[15] Walsh AW, Falk PJ, Thanassi J, et al. Comparison of the D-glutamate-adding enzymes from selected gram-positive and gram-negative bacteria. J Bacteriol. 1999;181(17):5395–5401.
[16] Gegnas LD, Waddell ST, Chabin RM, et al. Inhibitors of the bacterial cell wall biosynthesis enzyme MurD. Bioorg Med Chem Lett. 1998;8(13):1643–1648.
[17] Gobec S, Urleb U, Auger G, et al. Synthesis and biochemical evaluation of some novel N-acyl phosphono- and phosphinoalanine derivatives as potential inhibitors of the D-glutamic acid-adding enzyme. Die Pharmazie. 2001;56(4):295–297.
[18] Strancar K, Blanot D, Gobec S. Design, synthesis and structure–activity relationships of new phosphinate inhibitors of MurD. Bioorg Med Chem Lett. 2006;16:343–348.
[19] Auger G, van Heijenoort J, Blanot D, et al. Synthesis of N-Acetylmuramic acid derivatives as potential inhibitors of the D-glutamic acid-adding enzyme. J Prakt Chem. 1995;337(1):351–357.
[20] Sova M, Kovac A, Turk S, et al. Phosphorylated hydroxyethylamines as novel inhibitors of the bacterial cell wall biosynthesis enzymes MurC to MurF. Bioorg Chem. 2009;37(6):217–222.
[21] Pratviel-Sosa F, Acher F, Trigalo F, et al. Effect of various analogues of D-glutamic acid on the D-glutamate-adding enzyme from *Escherichia coli*. FEMS Microbiol Lett. 1994;115:223–228.
[22] Kotnik M, Humljan J, Contreras-Martel C, et al. Structural and functional characterization of enantiomeric glutamic acid

derivatives as potential transition state analogue inhibitors of MurD ligase. J Mol Biol. 2007;370(1):107–115.
[23] Humljan J, Kotnik M, Contreras-Martel C, et al. Novel naphthalene-N-sulfonyl-D-glutamic acid derivatives as inhibitors of MurD, a key peptidoglycan biosynthesis enzyme. J Med Chem. 2008; 51(23):7486–7494.
[24] Perdih A, Bren U, Solmajer T. Binding free energy calculations of N-sulphonyl-glutamic acid inhibitors of MurD ligase. J Mol Model. 2009;15(8):983–996.
[25] Zidar N, Tomaslc´ T, SInk R, et al. Discovery of novel 5-benzylidenerhodanine and 5-benzylidenethiazolidine-2,4-dione inhibitors of MurD ligase. J Med Chem. 2010;53(18):6584–6594.
[26] Zidar N, Tomasic T, Sink R, et al. New 5-benzylidenethiazolidin-4-one inhibitors of bacterial MurD ligase: design, synthesis, crystal structures, and biological evaluation. Eur J Med Chem. 2011; 46(11):5512–5523.
[27] Sosic I, Barreteau H, Simcic M, et al. Second-generation sulfonamide inhibitors of D-glutamic acid-adding enzyme: activity optimisation with conformationally rigid analogues of D-glutamic acid. Eur J Med Chem. 2011;46:2880–2894.
[28] Perdih A, Wolber G, Solmajer T. Molecular dynamics simulation and linear interaction energy study of D-Glu-based inhibitors of the MurD ligase. J Comput Aided Mol Des. 2013;27(8):723–738.
[29] Perdih A, Hrast M, Barreteau H, et al. Benzene-1,3-dicarboxylic acid 2,5-dimethylpyrrole derivatives as multiple inhibitors of bacterial Mur ligases (MurC-MurF). Bioorg Med Chem. 2014;22(15):4124–4134.
[30] Tomasc T, Sink R, Zidar N, et al. Dual inhibitor of MurD and MurE ligases from *Escherichia coli* and *Staphylococcus aureus*. ACS Med Chem Lett. 2012;3:626–630.
[31] Turk S, Kovac A, Boniface A, et al. Discovery of new inhibitors of the bacterial peptidoglycan biosynthesis enzymes MurD and MurF by structure-based virtual screening. Bioorg Med Chem. 2009;17(5):1884–1889.
[32] Simcic M, Pureber K, Kristan K, et al. A novel 2-oxoindolinylidene inhibitor of bacterial MurD ligase: enzyme kinetics, protein-inhibitor binding by NMR and a molecular dynamics study. Eur J Med Chem. 2014;83:92–101.
[33] Azam MA, Jupudi S, Saha N, et al. Combining molecular docking and molecular dynamics studies for modelling *Staphylococcus aureus* MurD inhibitory activity. SAR QSAR Environ Res. 2019;30(1):1–20.
[34] Azam MA, Jupudi S. Structure based virtual screening to identify inhibitors against *Staphylococcus aureus* MurD Enzyme. Stru Chem. 2019;1–11. DOI: 10.1007/s11224-019-01330-z
[35] Mahran MA, William S, Ramzy F, et al. Synthesis and in vitro evaluation of new benzothiazole berivatives as schistosomicidal agents. Molecules. 2007;12(3):622–633.
[36] Holsworth D, Waaler J, Machon O, et al. Azole derivatives as WTN pathway inhibitors. US Pat. 2012/US 8,883,827 A1, Aug. 16, Appl. No.: 13/376,202. PCT Filed: Jun. 7, 2010.
[37] Clinical and Laboratory Standard Institute (CLSI). Methods for dilution antibacterial susceptibility test for bacteria that grow aerobically, 7th ed. Approved Standard (MA7-A7); Clinical and Laboratory Standard Institute: Wayne. 2007. 27:133.
[38] Auger G, Martin L, Bertrand J, et al. Large-scale preparation, purification, and crystallization of UDP-N-acetylmuramoyl-L-alanine: D-glutamate ligase from *Escherichia coli*. Prot Express Purif. 1998; 13(1):23–29.
[39] Lanzetta PA, Alvarez LJ, Reinach PS, et al. An improved assay for nanomole amounts of inorganic phosphate. Anal Biochem. 1979; 100(1):95–97.
[40] Sastry MG, Adzhigirey M, Day T, et al. Protein and ligand preparation: parameters, protocols, and influence on virtual screening enrichments. J Comput Aided Mol Des. 2013;27:221–234.
[41] Jacobson MP, Pincus DL, Rapp CS, et al. A hierarchical approach to all-atom protein loop prediction. Proteins. 2004;55(2):351–367.
[42] Li J, Abel R, Zhu K, et al. The VSGB 2.0 Model: a next generation energy model for high resolution protein structure modelling. Proteins. 2011;79(10):2794–2812.
[43] Harder E, Damm W, Maple J, et al. OPLS3: A force field providing broad coverage of drug-like small molecules and protein. J Chem Theory Comput. 2016;12(1):281–296.
[44] Jorgensen WL, Madura JD. Temperature and size dependence for Monte Carlo simulations of TIP4P water. Mol Phys. 1985;56(6): 1381–1392.
[45] Lawrence CP, Skinner JL. Flexible TIP4P model for molecular dynamics simulation of liquid water. Chem Phys Lett. 2003;372(5-6):842–847.
[46] Essmann U, Perera L, Berkowit ML, et al. A smooth particle mesh Ewald method. J Chem Phys. 1995;103(19):8577–8593.
[47] Martyna GJ, Klein ML, Tuckerman M. Nose-Hoover chains: the canonical ensemble via continuous dynamics. J Chem Phys. 1992; 97(4):2635–2643.
[48] Martyna GJ, Tobias DJ, Klein ML. Constant-pressure molecular dynamics algorithms. J Chem Phys. 1994;101(5):4177–4189.